

COMMUNICATION

[View Article Online](#)
[View Journal](#)

Cite this: DOI: 10.1039/d5py00337g

Received 4th April 2025,

Accepted 3rd July 2025

DOI: 10.1039/d5py00337g

rsc.li/polymers

Group transfer polymerization by argon droplet flow for continuous and consistent production of well-defined polymers†

Ryo Takabayashi,^a Stephan Feser,^b Hiroshi Yonehara,^a Mamoru Hyodo,^c
Ilhyong Ryu^{c,d} and Takahide Fukuyama^e*

In search of a reliable flow polymerization, group transfer polymerization (GTP) of methyl methacrylate (MMA) using gas–liquid droplet flow by argon and fully continuous flow was compared. The \bar{D} values of polyMMA under the argon droplet flow were consistently lower than those of the fully continuous flow.

Flow reaction technology has expanded its applications to wider areas covering organic synthesis to polymer synthesis.^{1–5} Excellent efficiency in both mixing and heat transfer inherent to the high surface-to-volume ratio is the basis for allowing rapid reactions with the precise control of reaction time.^{6,7} Two decades ago, Yoshida's group reported on the flow radical polymerization of butyl acrylate, demonstrating for the first time that radical polymerization under conditions of flow resulted in the formation of polymers with lower polydispersity index (\bar{D}) values than those produced in a batch process, due to more efficient heat management of flow-micro-reactors.⁸ In flow polymer synthesis, the clogging of microflow reactors had been a primary concern. However, emerging reliable examples of continuous-flow polymerization systems have proved that they represent a practically useful repertoire for polymerization.^{9–11} An additional feature of interest to industries is a smaller footprint associated with flow chemical production for value-added compounds, such as active pharmaceutical ingredient (API) chemicals and functional polymers, which is consistent with the sustainable development goals (SDGs).^{12–15}

The synthesis and application of well-defined copolymers with low \bar{D} values have been extensively studied for decades with the goal of understanding their specific properties.^{16–18} As a result, a variety of di-block copolymers are now being used in many different industrial applications, *e.g.*, as adhesives, elastomers, surfactants, and pigment dispersants.^{19–22} Reversible deactivation radical polymerization (RDRP), such as atom transfer radical polymerization (ATRP), reversible addition fragmentation chain transfer (RAFT), and ionic polymerization are commonly used to prepare such well-defined copolymers.^{23–29} Despite limitations in monomer and solvent selection, group transfer polymerization (GTP), developed by Webster and his colleagues in 1983,³⁰ provides a convenient method for preparing well-defined polymers under mild reaction conditions.^{31,32}

While RDRP and ionic polymerization using flow reactors generally show lower \bar{D} values than those observed in batch reactors,^{33–40} they occasionally exhibit higher \bar{D} values.^{41–43} This is thought to be concerned with an intrinsic nature of fluid dynamics; a phenomenon in laminar flow occurs within the fluid in a situation where the central part of the fluid moves faster but the region near the walls moves slower, resulting in non-uniform residence time of the reaction mixture in the flow reactor (Fig. 1, top). The polymerization in the slow

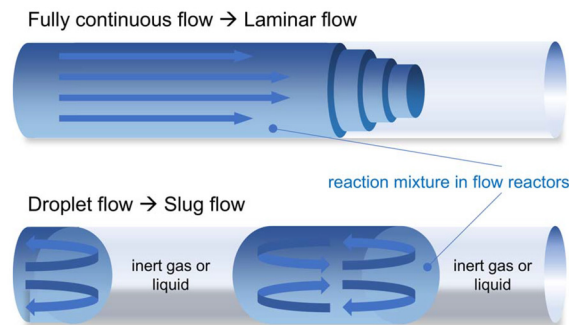


Fig. 1 Images of laminar flow (top) and slug flow (bottom) in flow reactors.

^aBYK Japan KK, 3-29 Ichigaya-Honmura-cho, Shinjuku-ku, Tokyo 162-0845, Japan

^bBYK-Chemie GmbH, Abelstrasse 45, 46483 Wesel, Germany

^cOrganization for Research Promotion, Osaka Metropolitan University, 1-1 Gakuen-cho Naka-ku, Sakai, Osaka 599-8531, Japan

^dDepartment of Applied Chemistry, National Yang Ming Chiao Tung University (NYCU), Hsinchu 30010, Taiwan

^eDepartment of Chemistry, Graduate School of Science, Osaka Metropolitan University, 3-3-138 Sugimoto-cho, Sumiyoshi-ku, Osaka, Osaka 558-8585, Japan.

E-mail: fukuyama@omu.ac.jp

† Electronic supplementary information (ESI) available. See DOI: <https://doi.org/10.1039/d5py00337g>

part can result in polymers with higher D values, thus resulting in worsened and inconsistent D values. To mitigate such a laminar flow effect in flow polymerization, the use of mixing-promoting devices such as static mixers⁴⁴ and zigzag-shaped reactors,⁴⁵ has been investigated in attempts to improve the quality of the obtained polymers.

On the other hand, droplet flow has attracted recent attention as a strategy for mitigating laminar flow effects, because it promotes the mixing in each tiny slug flow by causing circulating flows inside (Fig. 1, bottom).^{46–49} Reis *et al.* reported on ring-opening and RAFT polymerization that proceeded by gas-liquid droplet flow using argon, achieving lower D values than those with fully continuous flow.⁵⁰ Corrigan *et al.* reported that gas-liquid droplet flow using air yielded lower D values in the photoinduced electron/energy transfer-RAFT than fully continuous flow, even when the operating time became longer than 6 h.⁵¹ To the best of our knowledge, research on GTP in droplet flow has yet to be reported, and queerly, there is limited research on GTP even in fully continuous flow.⁵² This led us to study the flow GTP of methyl methacrylate (MMA) using argon-liquid droplet flow to compare the performance with fully continuous flow. The droplet flow polymerization showed lower D values than the fully continuous flow, to our delight. Interestingly, the D values remained constant even with the long operating time, which contrasts with the worsened D values in the case of the fully continuous flow which involves a long operating time.

We first conducted the GTP of MMA by batch or flow to determine how number average molecular weights (M_n) and D values of the obtained polyMMA varied (Table 1). Based on Kakuchi's protocol,⁵³ using dimethyl ketene methyl trimethylsilyl acetal (MTS) as an initiator and a 0.8 M hexane solution of 1-*tert*-butyl-4,4,4-tris(dimethylamino)-2,2-bis[tris(dimethylamino)-phosphoranylideneamino]-2A⁵,4A⁵-catenadi(phospha-

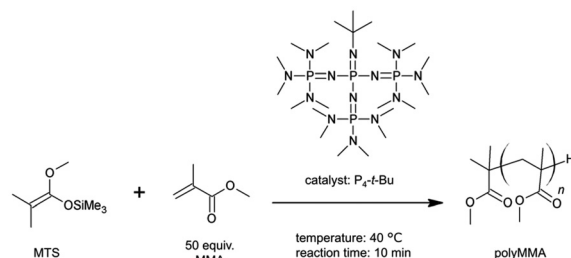
zene) (P_4 -*t*-Bu) as a catalyst, the GTP of MMA was conducted in propylene glycol monomethyl ether acetate (PEGMEA) as a solvent for 10 min at 40 °C. To investigate the influence of the reaction scale on M_n and D values, batch reactions were performed either on a 3 g scale of MMA using a 30 mL test tube or on a 17 g scale of MMA in a 100 mL flask. Although the small-scaled batch reaction in the 30 mL test tube yielded polyMMA with an M_n value of 6833 and $D = 1.46$, that on the larger scale conducted in the 100 mL flask yielded polyMMA with an M_n of 6090 and $D = 1.52$ (entries 1 and 2 in Table 1). These results indicate that control of the batch reactions of GTP was slightly lost when the reaction was scaled up, possibly because of less efficient mixing and/or heat transfer. Next, fully continuous and argon droplet flow reactions were carried out (for the device setting, see the full line and dashed line in Fig. 4). The first 30 min-elute was discarded, and samples were then collected for 10 min. While the fully continuous flow showed an M_n of 5619 with $D = 1.56$, the droplet flow showed an M_n of 6349 with $D = 1.45$, showing slight improvement in the droplet flow in terms of D values (entries 3 and 4 in Table 1).

Because the study reported by Corrigan *et al.* concerning fully continuous flow did not show consistent D values as the operating time became longer,⁵¹ we carried out the experiment in which the operating time was extended to 110 min (Fig. 2). Indeed, the D values increased gradually, and after 110 min of operating time, the fully continuous flow gave an M_n of 5542 with a D value of 1.98. In contrast, the droplet flow gave an M_n of 6096 with a consistent D value of 1.41. GPC charts with the longer operating time for the fully continuous flow showed a growing shoulder in the higher molecular part (see an arrow, Fig. 3(a)), which was not observed in the droplet flow (Fig. 3(b)). Presumably, the ununified residence time inherent to laminar continuous flow allows for the slowly moving part

Table 1 GTP of MMA in batch, fully continuous and droplet flow^a

Entry	Reactor	Theo. M_n^b (g mol ⁻¹)	M_n^c (g mol ⁻¹)	D	Conv. ^d (%)
1	Batch (3 g scale)	5036	6833 (±87)	1.46 (±0.01)	99% (±0)
2	Batch (17 g scale)	4969	6090 (±99)	1.52 (±0.00)	97% (±0)
3	Fully continuous flow ^e	5036	5619 (±82)	1.56 (±0.03)	99% (±0)
4	Droplet flow ^e	5036	6349 (±312)	1.45 (±0.01)	99% (±0)

^a $[MMA]_0/[MTS]_0/[P_4-t-Bu] = 50/1/0.001$, $(MMA + MTS)/(PEGMEA) = 30/70$ in weight. Reactions were carried out three times, and the standard deviations are reported in the parentheses. ^b The theoretical M_n was calculated as follows: $[MMA]_0/[MTS]_0 \times (MW \text{ of MMA, } 100.1) + (MW \text{ of the residual initiator in the polymer, } 102.1) \times \text{Conv.}(\%)$. ^c Measured by gel permeation chromatography. ^d Measured by gas chromatography. ^e The flow reactors' length was 9.0 m with an i.d. of 2.0 mm. The first 30 min-elute was discarded, and then the samples were collected for 10 min.



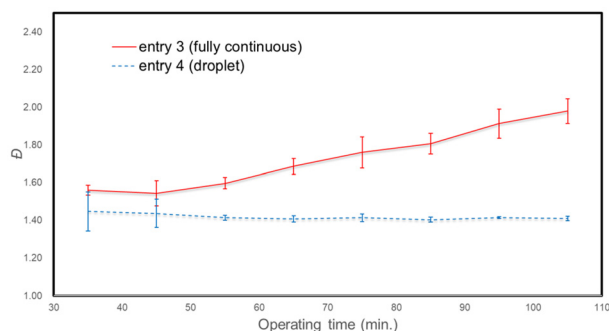


Fig. 2 Shifts of \bar{D} values of the fully continuous and droplet flow in the long operating time (31–110 m). Reactions were carried out three times, and the standard deviations are described in the error bars.

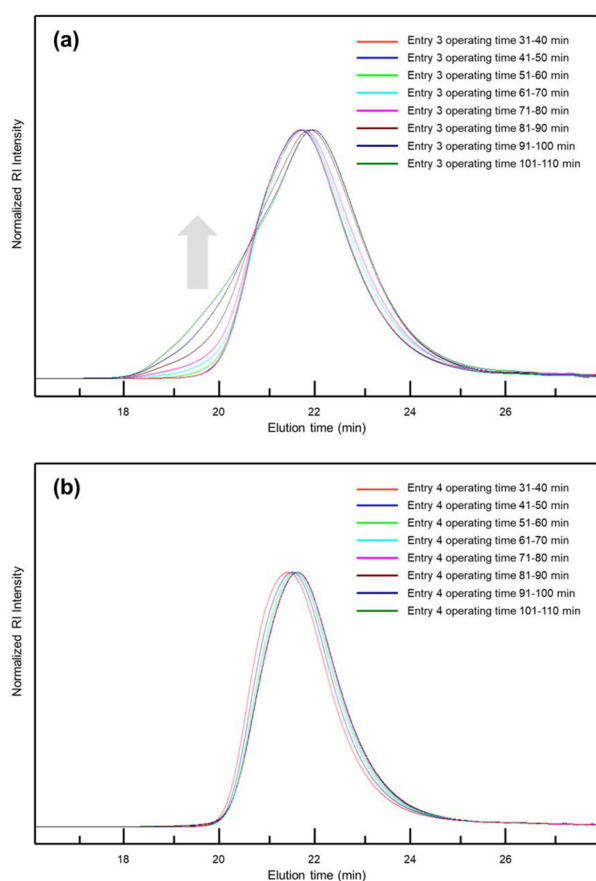


Fig. 3 GPC charts of the fully continuous flow (a) and the droplet flow (b) in GTP of MMA in an operating time range of 31–110 min.

of the reaction mixture to grow a long polymer chain. In contrast, the argon droplet flow, free of laminar flow, can consistently perform GTP with \bar{D} values as low as that obtained in the very small batch reaction, even in the long operating time.

To gain some additional insights into the effectiveness of argon droplet flow over continuous flow, the GTP of MMA was performed with different flow settings: (a) internal diameter (i.

d.) of flow reactors, (b) flow rates, (c) the degree of polymerization of MMA and (d) dilution of the reaction mixture. The results are summarized in Fig. 4. We first investigated the effect of i.d. using three sets of 9.0 m PFA tubes with i.d. values of 1.6, 2.0, and 3.0 mm, respectively (Fig. 4(a)). The residence time was maintained constant at 10 min, and the samples were collected every 10 min for 11–110 min. The droplet flow in each i.d. showed consistent \bar{D} values after 30 min to 110 min irrespective of diameter size (the blue marks in Fig. 4(a)). Fully continuous flow, however, showed a gradual increase of the \bar{D} values as the operating time became longer (the red marks in Fig. 4(a)). This is particularly true for reactions with the smallest i.d. of 1.6 mm, in which a notable increase in the \bar{D} values was observed. It is known that laminar flow occurs when the Reynolds number (Re) is small and smaller i.d. contributes to making Re smaller (eqn (1)), resulting in ununified residence time of the continuous flow.⁵⁴

$$Re = UD/\nu \quad (1)$$

Here, U and ν represent the velocity and kinematic viscosity of the fluid in the tubular reactor, respectively, and D represents the inside diameter (i.d.) of the tubular reactor.

The effect of the flow rate on \bar{D} values was also investigated, using 4.5, 9.0, and 18.0 m PFA tubes with an i.d. of 2.0 mm (Fig. 4(b)). To unify the residence time to 10 min, the flow rates were set at 1.40 mL min⁻¹ with length = 4.5 m, 2.82 mL min⁻¹ with length = 9.0 m, and 5.66 mL min⁻¹ with length = 18.0 m, respectively. Droplet flow with each length of the flow reactor showed lower \bar{D} values than the corresponding values for fully continuous flow. The most undesirable \bar{D} values were observed in the slowest flow rates with a reactor length of 4.5 m (the red and blue circles in Fig. 4(b)). This observation is rational because Re was the smallest due to the slowest velocity. As there were no significant differences in \bar{D} values among the various flow rates in droplet flow, we assume that the mixing effect of slug flow was sufficient at these flow rates. Further investigation into the correlations between the flow rates and the \bar{D} values of the obtained polymers is underway.

The degrees of polymerization and \bar{D} values were also investigated by using three $[MMA]_0/[MTS]_0$ values, 25/1, 50/1, and 75/1, for which the theoretical molecular weights are 2604, 5108, and 7610, respectively (Fig. 4(c)). Interestingly, in the case of $[MMA]_0/[MTS]_0 = 25/1$, almost no differences in \bar{D} values were observed between the fully continuous and droplet flow, after reaching the consistent status in 60 min (the red and blue circles in Fig. 4(c)). On the other hand, in the case of $[MMA]_0/[MTS]_0 = 75/1$, significant differences in \bar{D} values were observed for 110 min which showed a $\bar{D} = 1.64$ for droplet flow and $\bar{D} = 2.00$ for fully continuous flow (the blue and red diamonds in Fig. 4(c)). A similar tendency was observed in the case of $[MMA]_0/[MTS]_0 = 50/1$ (the blue and red squares in Fig. 4(c)). Increased ratios of $[MMA]_0/[MTS]_0$ require a longer reaction time, and, in such cases, the droplet flow mitigated the laminar flow effect and allowed the reaction mixture to



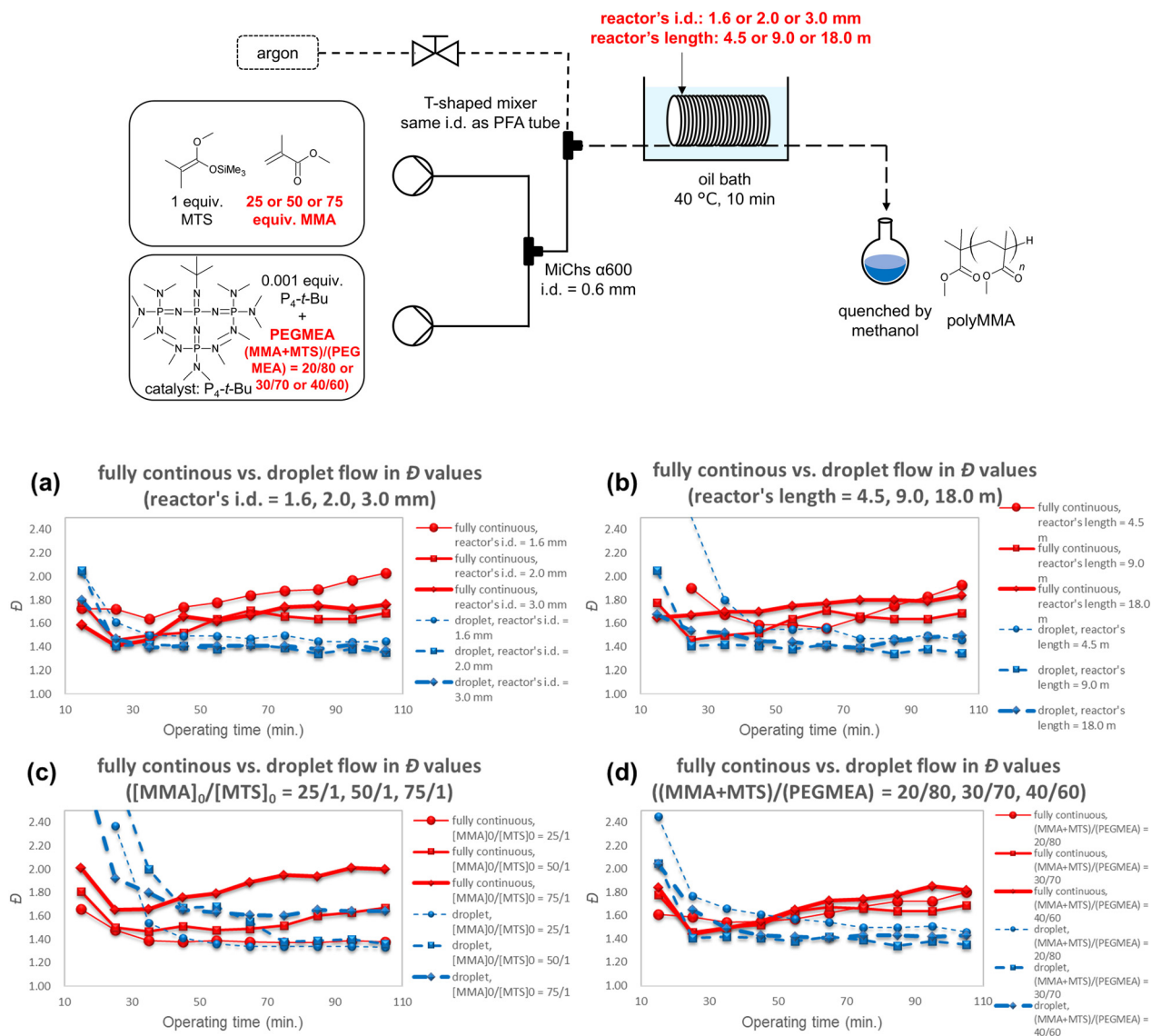


Fig. 4 Comparison of the GTP of MMA between fully continuous and droplet flow with various settings. (a) $[MMA]_0/[MTS]_0/[P_4-t-Bu] = 50/1/0.001$, $(MMA + MTS)/(PEGMEA) = 30/70$ in weight, flow length: 9.0 m with i.d. of 1.6, 2.0, and 3.0 mm, (b) $[MMA]_0/[MTS]_0/[P_4-t-Bu] = 50/1/0.001$, $(MMA + MTS)/(PEGMEA) = 30/70$ in weight, flow length: 4.5, 9.0, and 18.0 m with i.d. of 2.0 mm. (c) The reaction was conducted at 60 °C instead of 40 °C. $[MMA]_0/[MTS]_0/[P_4-t-Bu] = 25/1/0.001$, 50/1/0.001, and 75/1/0.001, $(MMA + MTS)/(PEGMEA) = 30/70$ in weight, flow length: 9.0 m with i.d. of 2.0 mm (d) $[MMA]_0/[MTS]_0/[P_4-t-Bu] = 50/1/0.001$, $(MMA + MTS)/(PEGMEA) = 20/80$, 30/70, and 40/60 in weight, flow length: 9.0 m with i.d. of 2.0 mm.

react more uniformly than was the case for fully continuous flow.

The viscosity effects of the reaction mixture in flow reactors on D values were also investigated by changing $(MMA + MTS)/(PEGMEA) = 40/60$, 30/70, and 20/80 in weight (Fig. 4(d)). D values were lower in the case of droplet flow than those in the fully continuous flow in 110 min in all cases (the red and blue marks in Fig. 4(d)). All data of D values, M_n , and monomer conversions with different sampling times are available in the ESI.†

Encouraged by these promising results, we next carried out scalable synthesis using argon droplet flow (Fig. 5). The reaction conditions were $[MMA]_0/[MTS]_0 = 50/1$ (theoretical mole-

cular weight is 5108) with $(MMA + MTS)/(PEGMEA) = 30/70$ in weight. The residence time was 10 min at 40 °C with a flow rate of 3.18 mL min⁻¹. In 30 min, M_n became 6107 with $D = 1.34$ and monomer conv. = 99%, and consistent values were maintained, resulting in $M_n = 5889$ with $D = 1.34$ and monomer conv. = 98% over 10 h operating time (Fig. 5), giving 0.5 kg of polyMMA. These data suggest that the present argon droplet protocol for GTP for scalable synthesis using a long operating time has potential for use.

We then investigated the use of GTP to give a di-block copolymer of MMA and butyl methacrylate (BMA) in argon droplet flow (Scheme 1). We planned to produce a di-block of $[MMA]_0/[BMA]_0/[MTS]_0 = 50/10/1$ in PEGMEA, giving a di-block copoly-



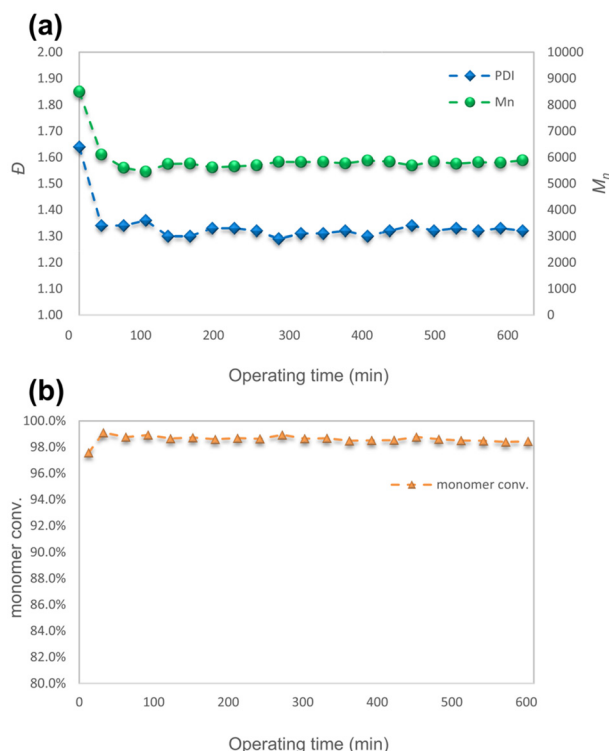


Fig. 5 Droplet flow of GTP for a 600 min operating time. $[MMA]_0/[MTS]_0/[P_4-t-Bu] = 50/1/0.001$, $(MMA + MTS)/(PEGMEA) = 30/70$ in weight, flow length: 9.0 m with i.d. of 3.0 mm, (a) \bar{D} values and M_n , and (b) monomer conversion with different sampling times.

mer having a theoretical molecular weight of 6530. The first MMA block was polymerized with a residence time of 10 min at 40 °C, and the second block BMA was polymerized with a residence time of 19 min. To improve the monomer conversion of BMA, the catalyst $[P_4-t-Bu] = 0.001$ against $[MTS]_0$ was added twice: once at the start of the first block polymerization and again at the start of the second. The first 29 min-elute was discarded, and the samples were collected at 29 min intervals

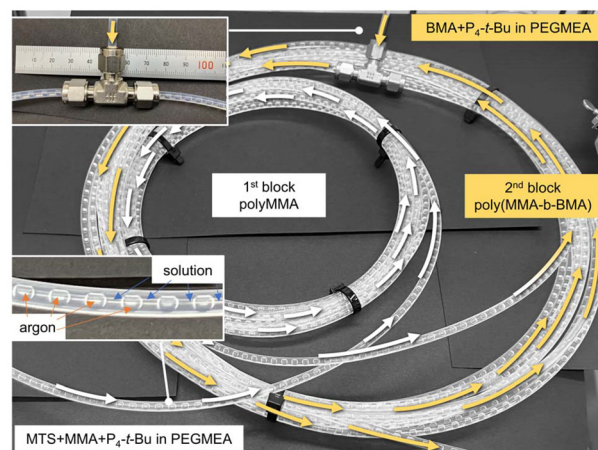
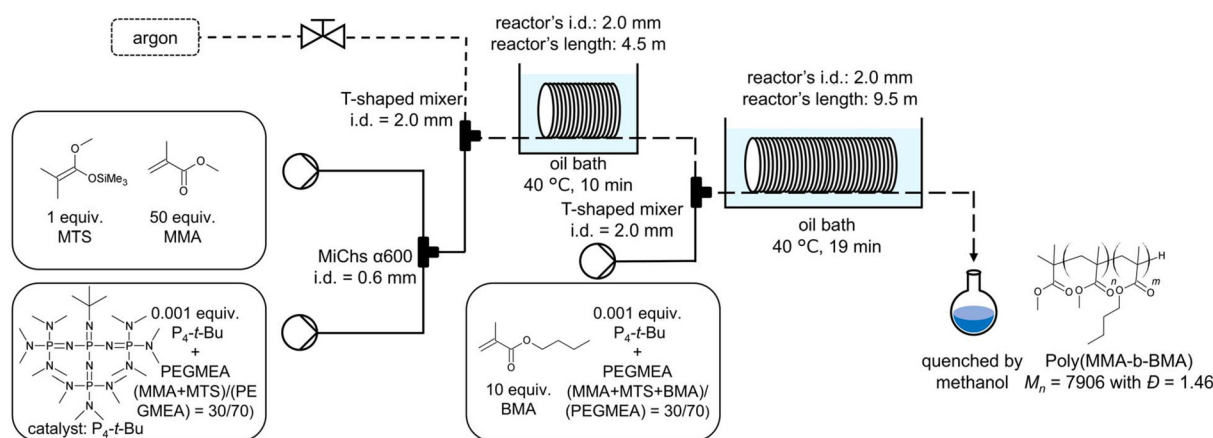


Fig. 6 Appearance of droplet flow on poly(MMA-*b*-BMA) by GTP. Flow length: 4.5 m for the 1st block and 9.5 m for the 2nd block with i.d. of 2.0 mm. The liquid flow rates were 0.71 mL min⁻¹ for the 1st block and 0.19 mL min⁻¹ for the 2nd block. This picture was taken without heating in an oil bath.

over a period of 29–290 min. When the second monomer BMA in PEGMEA was used, the size of the slug became slightly larger (Fig. 6). The obtained poly (MMA-*b*-BMA) was the desired di-block polymer: $M_n = 7906$ with $\bar{D} = 1.46$, and MMA conv. = 99% and BMA conv. = 99% after 270 min of operating time. These findings suggest that the argon droplet protocol is applicable for preparing di-block copolymers. All data on \bar{D} values, M_n , and monomer conversions with different sampling times are available in the ESI.†

Conclusions

In summary, we report on an investigation of the GTP of MMA using fully continuous and argon droplet flow. The findings show that the \bar{D} values for continuous flow are comparable



Scheme 1 Synthesis of poly(MMA-*b*-BMA) in droplet flow. $[MMA]_0/[BMA]_0/[MTS]_0/[P_4-t-Bu] = 50/10/1/(0.001 + 0.001)$, $(MMA + BMA + MTS)/(PEGMEA) = 30/70$ in weight.



those of poly-MMA with argon droplet flow when the operating time was short, but the D values became higher for a longer operating time. On the other hand, lower and consistent D values were found for droplet flow, even in the case of a longer operating time. We also demonstrated that argon droplet flow gave polymers with lower D values, especially in cases where the i.d. of flow reactors was smaller, with a slower flow rate of the reaction mixtures in flow reactors, even in the case of a higher degree of polymerization. This argon droplet protocol can produce 0.5 kg polyMMA with $D \sim 1.3$ over 10 hours of operating time. We also conclude that the droplet flow protocol can be successfully used for preparing poly(MMA-*b*-BMA) by GTP. The argon droplet process represents a reliable method for use in the flow-controlled polymerization of well-defined polymers. We are currently investigating the application of this process to some other controlled polymerization systems.

Conflicts of interest

There are no conflicts to declare.

Data availability

The data supporting this article have been included as part of the ESI.†

Acknowledgements

TF and IR wish to thank JSPS KAKENHI for providing funding for this work (24K08433 and 19H02722). IR thanks NSTC (MOST112-2113-MA49-013) and the Center for Emergent Functional Matter Science at NYCU for additional support (111W20253).

References

- 1 T. Wirth, *Microreactors in Organic Chemistry and Catalysis*, Wiley-VCH, Weinheim, 2nd edn, 2013.
- 2 K. F. Jensen, B. J. Reizman and S. G. Newman, *Lab Chip*, 2014, **14**, 3206–3212.
- 3 J. Wegner, S. Ceylan and A. Kirschning, *Adv. Synth. Catal.*, 2012, **354**, 17–57.
- 4 B. Gutmann, D. Cantillo and C. O. Kappe, *Angew. Chem., Int. Ed.*, 2015, **54**, 6688–6728.
- 5 J. Jiao, W. Nie, T. Yu, F. Yang, Q. Zhang, F. Aihemaiti, T. Yang, X. Liu, J. Wang and P. Li, *Chemistry*, 2021, **27**, 4817–4838.
- 6 J. Yoshida, H. Kim and A. Nagaki, *ChemSusChem*, 2011, **4**, 331–340.
- 7 R. L. Hartman, J. P. McMullen and K. F. Jensen, *Angew. Chem., Int. Ed.*, 2011, **50**, 7502–7519.
- 8 T. Iwasaki and J. Yoshida, *Macromolecules*, 2005, **38**, 1159–1163.
- 9 A. Nagaki and J. Yoshida, in *Advances in Polymer Science*, Springer International Publishing, Cham, 2012, pp. 1–50.
- 10 M. H. Reis, F. A. Leibfarth and L. M. Pitet, *ACS Macro Lett.*, 2020, **9**, 123–133.
- 11 N. Zaquen, M. Rubens, N. Corrigan, J. Xu, P. B. Zetterlund, C. Boyer and T. Junkers, *Prog. Polym. Sci.*, 2020, **107**, 101256.
- 12 T. Junkers, *Macromol. Chem. Phys.*, 2017, **218**, 1600421.
- 13 D. Kohlmann, M.-C. Chevreil, S. Hoppe, D. Meimaroglou, D. Chapron, P. Bourson, C. Schwede, W. Loth, A. Stammer, J. Wilson, P. Ferlin, L. Falk, S. Engell and A. Durand, *Macromol. React. Eng.*, 2016, **10**, 339–353.
- 14 M. Baumann, T. S. Moody, M. Smyth and S. Wharry, *Org. Process Res. Dev.*, 2020, **24**, 1802–1813.
- 15 B. J. Doyle, P. Elsner, B. Gutmann, O. Hannaerts, C. Aellig, A. Macchi and D. M. Roberge, *Org. Process Res. Dev.*, 2020, **24**, 2169–2182.
- 16 W. A. Braunecker and K. Matyjaszewski, *Prog. Polym. Sci.*, 2007, **32**, 93–146.
- 17 N. Corrigan, K. Jung, G. Moad, C. J. Hawker, K. Matyjaszewski and C. Boyer, *Prog. Polym. Sci.*, 2020, **111**, 101311.
- 18 R. B. Grubbs and R. H. Grubbs, *Macromolecules*, 2017, **50**, 6979–6997.
- 19 H. Sajjad, W. B. Tolman and T. M. Reineke, *ACS Appl. Polym. Mater.*, 2020, **2**, 2719–2728.
- 20 J. Feng, Z. Wang, P. Tang, L. Liu, S. Chen and F. Jiang, *Polymer*, 2023, **264**, 125543.
- 21 A.-V. Ruzette and L. Leibler, *Nat. Mater.*, 2005, **4**, 19–31.
- 22 F. L. Duivenvoorde, J. Laven and R. van der Linde, *Prog. Org. Coat.*, 2002, **45**, 127–137.
- 23 K. Matyjaszewski and J. Xia, *Chem. Rev.*, 2001, **101**, 2921–2990.
- 24 K. Matyjaszewski, *Macromolecules*, 2012, **45**, 4015–4039.
- 25 G. Moad, E. Rizzardo and S. H. Thang, *Aust. J. Chem.*, 2012, **65**, 985.
- 26 S. Perrier, *Macromolecules*, 2017, **50**, 7433–7447.
- 27 N. Hadjichristidis, M. Pitsikalis, S. Pispas and H. Iatrou, *Chem. Rev.*, 2001, **101**, 3747–3792.
- 28 S. Aoshima and S. Kanaoka, *Chem. Rev.*, 2009, **109**, 5245–5287.
- 29 A. Hirao, R. Goseki and T. Ishizone, *Macromolecules*, 2014, **47**, 1883–1905.
- 30 O. W. Webster, W. R. Hertler, D. Y. Sogah, W. B. Farnham and T. V. RajanBabu, *J. Am. Chem. Soc.*, 1983, **105**, 5706–5708.
- 31 O. W. Webster, in *Advances in Polymer Science*, Springer Berlin Heidelberg, Berlin, Heidelberg, 2003, pp. 1–34.
- 32 K. Fuchise, Y. Chen, T. Satoh and T. Kakuchi, *Polym. Chem.*, 2013, **4**, 4278.
- 33 T. Noda, A. J. Grice, M. E. Levere and D. M. Haddleton, *Eur. Polym. J.*, 2007, **43**, 2321–2330.
- 34 M. Müller, M. F. Cunningham and R. A. Hutchinson, *Macromol. React. Eng.*, 2008, **2**, 31–36.
- 35 I. Ryu, A. Studer, T. Fukuyama and Y. Kajihara, *Synthesis*, 2012, **44**, 2555–2559.



- 36 R. Takabayashi, S. Feser, H. Yonehara, I. Ryu and T. Fukuyama, *Polym. Chem.*, 2023, **14**, 4515–4520.
- 37 C. Diehl, P. Laurino, N. Azzouz and P. H. Seeberger, *Macromolecules*, 2010, **43**, 10311–10314.
- 38 W. Liu, Q. Li, Y. Zhang, T. Liu, L. Wang, H. Li and Y. Hu, *J. Flow Chem.*, 2021, **11**, 867–875.
- 39 A. Nagaki, Y. Tomida and J. Yoshida, *Macromolecules*, 2008, **41**, 6322–6330.
- 40 F. Wurm, D. Wilms, J. Klos, H. Löwe and H. Frey, *Macromol. Chem. Phys.*, 2008, **209**, 1106–1114.
- 41 C. H. Hornung, C. Guerrero-Sanchez, M. Brasholz, S. Saubern, J. Chiefari, G. Moad, E. Rizzardo and S. H. Thang, *Org. Process Res. Dev.*, 2011, **15**, 593–601.
- 42 J. P. Russum, C. W. Jones and F. J. Schork, *Macromol. Rapid Commun.*, 2004, **25**, 1064–1068.
- 43 R. M. Paulus, T. Erdmenger, C. R. Becer, R. Hoogenboom and U. S. Schubert, *Macromol. Rapid Commun.*, 2007, **28**, 484–491.
- 44 F. G. Lueth, W. Pauer and H.-U. Moritz, *Macromol. Symp.*, 2013, **333**, 69–79.
- 45 K. Iida, T. Q. Chastek, K. L. Beers, K. A. Cavicchi, J. Chun and M. J. Fasolka, *Lab Chip*, 2009, **9**, 339–345.
- 46 J. P. Russum, C. W. Jones and F. J. Schork, *AIChE J.*, 2006, **52**, 1566–1576.
- 47 H. Song, D. L. Chen and R. F. Ismagilov, *Angew. Chem., Int. Ed.*, 2006, **45**, 7336–7356.
- 48 J. Song, S. Zhang, K. Wang and Y. Wang, *J. Taiwan Inst. Chem. Eng.*, 2019, **98**, 78–84.
- 49 Y. Zhou, Y. Gu, K. Jiang and M. Chen, *Macromolecules*, 2019, **52**, 5611–5617.
- 50 M. H. Reis, T. P. Varner and F. A. Leibfarth, *Macromolecules*, 2019, **52**, 3551–3557.
- 51 N. Corrigan, L. Zhernakov, M. H. Hashim, J. Xu and C. Boyer, *React. Chem. Eng.*, 2019, **4**, 1216–1228.
- 52 M. Hasegawa, M. Imada, H. Fukutome and H. Ando, *JP Pat*, 7390201B2, 2023.
- 53 T. Kakuchi, Y. Chen, J. Kitakado, K. Mori, K. Fuchise and T. Satoh, *Macromolecules*, 2011, **44**, 4641–4647.
- 54 K. Avila, D. Moxey, A. de Lozar, M. Avila, D. Barkley and B. Hof, *Science*, 2011, **333**, 192–196.

